Chinese Journal of Aeronautics, (2021), 34(10): 81–90

Chinese Society of Aeronautics and Astronautics
& Beihang University

Chinese Journal of Aeronautics

cja@buaa.edu.cn
www.sciencedirect.com

Initiation characteristics of oblique detonation waves from a finite wedge under argon dilution

Ying GAO [a], Haoyang LI [b], Gaoxiang XIANG [b,*], Shunhao PENG [b]

[a] Department of Teaching Quality Evaluation, Yan'an University, Yan'an 716000, China
[b] School of Mechanics, Civil Engineering & Architecture, Northwestern Polytechnical University, Xi'an 710129, China

Received 10 July 2020; revised 3 August 2020; accepted 19 October 2020
Available online 9 January 2021

KEYWORDS

Oblique detonation;
Finite wedge;
Argon dilution;
Initiation characteristics;
Numerical simulation

Abstract In this paper, the flow field characteristics of Oblique Detonation Waves (ODWs) induced by a finite wedge under argon dilution are studied by solving the Euler equations with a detailed chemical model of hydrogen and air. First, the effects of the expansion waves, argon concentration, geometric parameters, and Mach number on the ODW are discussed. The results show that the changes of these parameters may make the oblique detonation not be initiated. Then, the ODW initiation criterion of the finite wedge is summarized, as the characteristic length of the induction zone L_C and the characteristic length of the oblique wedge L_W meet the condition $L_C/L_W < 1$, the initiation of the ODW occurs; otherwise, it does not occur. What's more, the Constant Volume Combustion (CVC) theory is applied to study the characteristic length of induction zone. It is found that CVC theory is more suitable for the "smooth transition" type of ODW flow field, the theoretical and numerical characteristic length in induction regions are in good agreement. This work is of great significance for the design of oblique detonation engines for hypersonic vehicles.

1. Introduction

Detonation combustion can release fuel energy in a microsecond, and the detonation wave propagation speed can reach values on the order of kilometers per second, which is suitable for the hypersonic propulsion systems of new-generation aircraft.[1–3] The detonation engines include the Pulse Detonation Engine (PDE),[4] the Rotating Detonation Engine (RDE)[5–7] and the Oblique Detonation Engine (ODE).[8,9] Compared with the common scramjet,[10–13] the ODE can maintain a higher combustion efficiency at a higher flight Mach number. In addition, the ODE is lightweight and easy to start repeatedly, and has a short combustion chamber length and small flight resistance; thus, it has attracted worldwide interest. At present, one of the main ways to generate oblique shock waves is with the use of a wedge to induce oblique detonation. Related investigations are helpful for the realization of oblique detonation engines and their applications in practical engineering as soon as possible.

* Corresponding author.
E-mail address: xianggx@nwpu.edu.cn (G. XIANG).
Peer review under responsibility of Editorial Committee of CJA.

Production and hosting by Elsevier

https://doi.org/10.1016/j.cja.2020.11.013
1000-9361

There are three methods by which to study ODW, namely gas detonation theory, hypersonic experiment, and computational fluid dynamics approach. The classical theories include CJ (Chapman-Jouguet) theory and the ZND (Zel'dovich-von Neumann-Döring) model,[14–16] which can be respectively used to determine the velocity and structure of a detonation wave. The experimental techniques include the hypervelocity projectile and the shock tube, which are combined with the high-speed photography, schlieren technology, and laser-induced fluorescence technology. The high-frequency pressure measurements are usually use the piezoelectric pressure sensor and the piezoresistive pressure sensor. In many experiments, a variety of methods are adopted to study Oblique Detonation Waves (ODWs). As a commonly used method, the numerical method has some limitations, but its cost is relatively low. When the discrete scheme, chemical model and physical model are selected appropriately, the results can be used to accumulate experience for the study of ODWs.

A substantial amount of research on oblique detonation induced by oblique shock waves has been carried out by scholars both domestically and internationally, and includes investigations of the structure of ODW,[17–21] cell lattice characteristics,[22,23] initiation mechanisms,[24–26] stability,[27–30] and unsteady non-uniform flow.[31,32] Li et al.[33] found that the flow field structure of oblique detonation induced by a wedge includes an oblique shock wave, reaction zone, deflagration wave, and subsequent ODW. Viguier et al.[34] confirmed the existence of the ODW structure, Teng et al.[35] studied the initiation structure of an ODW induced by a semi-infinite wedge under different incoming Mach numbers, temperatures, and wedge angles. It was found that the initiation structure of the ODW can be categorized into two types, namely "smooth transition" and "abrupt transition". Radulescu et al.[36] confirmed via numerical calculation and experimental results that the addition of argon as a diluent gas in acetylene/oxygen can make the detonation structure more stable. Wang et al.[37] used a hybrid Eulerian-Lagrangian method to study the ODW in two-phase kerosene-air mixtures over a wedge, and the initiation feature of the two-phase oblique detonation was elucidated. Zhang et al.[38] further verified the failure mechanism of high-concentration argon dilution gas on the surface curvature of detonation waves. In the oblique detonation engine, a wedge is needed to generate an oblique shock wave, which can induce the initiation of an ODW. In previous research, highly simplified semi-infinite wedge surfaces were used, and the influences of expansion waves and other boundaries were not considered. However, in real scenarios, the combustion chamber of the ODE is a confined space for the ODW, and cannot be infinitely extended after initiation. If the location of the expansion wave is sufficiently upstream, the oblique detonation will not be initiated.[25,39] To make the detonation wave more stable, it is necessary to study the ODW structure induced by a finite wedge in argon dilution, which plays an important role in the design of ODEs.

In this paper, the initiation mechanism of the effect of a finite wedge on oblique detonation in a hydrogen/air mixture diluted with different concentrations of argon is analyzed in detail. The mathematical and physical models are described in Section 2. In Section 3, the effects of the wedge length, argon concentration, and Mach number on the initiation characteristics, wave structure, temperature, and pressure distribution of oblique detonation are studied, and the ODW initiation criterion of a finite wedge is proposed and verified. Section 4 summarizes the main conclusions of this work.

2. Mathematical and physical models

Fig. 1 presents the computational sketch of the oblique detonation. The left boundary is the free stream condition, the initial temperature T_∞ is set as 300 K, the initial pressure p_∞ = 101325.0 Pa, the incoming Mach number Ma_∞ = 7.0–10.0, the premixed gas is hydrogen/air with an equivalence ratio of 1 and argon with different concentrations. The shadow area represents a solid wall, the dotted line and the upper boundary of the shadow area constitute the calculation domain, the wedge surface is a sliding solid wall boundary, and the rest of the boundary is a first-order zero-gradient free boundary. L_W represents the length of the oblique wedge that originating from the leading edge to the turning point. L_C is defined as the characteristic length of induction zone that originating from the leading edge to the location of the deflagration. The wedge angle is 25°, and the solid wall boundary at the exit is parallel to the incoming flow boundary.[8,31] Under high Mach number flow conditions, an oblique shock wave will be formed at the front of the wedge. The wedge surface will turn at a certain point and the expansion wave will form at the turning point, which will affect the initiation structure of the ODW. If the flow condition and wedge length are suitable, the ODW will be induced to initiate and an ODW and slip line will be formed. In this research, the initial location of the wedge surface is x = 1 mm, and the mesh size is 25 μm.

This paper solves the 2D multi-species Euler equations,[40,41] which can be written as:

$$\frac{\partial \boldsymbol{U}}{\partial t}+\frac{\partial \boldsymbol{F}}{\partial x}+\frac{\partial \boldsymbol{G}}{\partial y}=\boldsymbol{S} \tag{1}$$

where

$$\boldsymbol{U}=\begin{bmatrix}\rho_1\\ \rho_2\\ \vdots\\ \rho_n\\ \rho u\\ \rho v\\ e\end{bmatrix},\boldsymbol{F}=\begin{bmatrix}\rho_1 u\\ \rho_2 u\\ \vdots\\ \rho_n u\\ \rho u^2+p\\ \rho uv\\ (e+p)u\end{bmatrix},\boldsymbol{G}=\begin{bmatrix}\rho_1 v\\ \rho_2 v\\ \vdots\\ \rho_n v\\ \rho uv\\ \rho v^2+p\\ (e+p)v\end{bmatrix},\boldsymbol{S}=\begin{bmatrix}\omega_1\\ \omega_2\\ \vdots\\ \omega_n\\ 0\\ 0\\ 0\end{bmatrix} \tag{2}$$

In the above equations, the subscript i (i = 1, 2, …, n) represents the ith species; p is the gas pressure; ω_i is the species' specific mass production rate. The total density ρ and total specific energy e can be calculated by

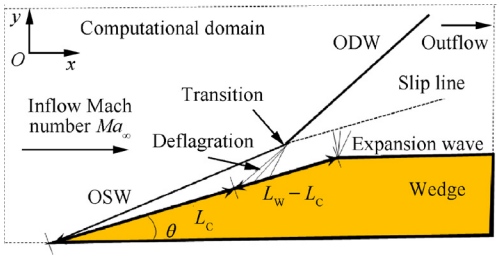

Fig. 1 Sketch of oblique detonation simulation.

$$\rho = \sum_{i=1}^{n} \rho_i, e = \rho h - p + \frac{1}{2}\rho(u^2 + v^2) \tag{3}$$

where u and v are the velocity in the x and y-direction, h is the specific enthalpy and can be written as $h = \sum_{i=1}^{n} \rho_i h_i / \rho$. The equation of state is $p = \sum_{i=1}^{n} \rho_i \frac{R_0}{W_i} T$, W_i is the molecular weight, R_0 is the gas constant, and T is the gas temperature.

The governing equations are discretized by an AUSMPW + scheme[42] and the thermodynamics properties of the chemical species are evaluated with 9-coefficient NASA polynomial representations.[43] H_2-Air-Ar elementary reactions model with 10 species (H_2, O_2, H, O, OH, HO_2, H_2O_2, H_2O, N_2, Ar) is adopted as the chemical reaction model. As is indicted in previous investigations conducted by Teng et al.,[40,41] the grid resolution 0.025 mm is enough to capture the wave structure, which is employed in every case in this paper.

3. Numerical results and discussion

3.1. Effects of expansion waves on ODW

Fig. 2(a) presents the structures of the ODWs of the finite wedge surface (above) and infinite wedge surface (below) under the condition of a 50% argon concentration. It can be seen from the figure that the main wave structures of the ODWs from the finite wedge and infinite wedge are the same; both are first formed in front of the wedge, and the detonation wave then converges at the end of the induction area, interacting with the incident shock wave. The ODW will be formed after initiation when reaching certain conditions. The expansion waves formed at the inflection point of the wedge affect the downstream flow field behind the inflection point, but has little influence on the upstream flow field before the inflection point. Fig. 2(b) presents the temperature and pressure distributions along the wall boundary of Fig. 2(a), in which the solid line represents the infinite wedge and the dotted line represents the finite wedge. The sudden increases in temperature and pressure at x = 1 mm are due to the compression of the incoming flow by the oblique shock wave in front of the wedge. The second sudden increases in the temperature and pressure near x = 6 mm are due to the compression of the deflagration wave. When the airflow reaches the inflection point of the wedge, the temperature and pressure of the finite wedge decrease sharply under the influence of the expansion wave.

In this work, the length of the induction zone is used to quantitatively study the initiation characteristics of the ODW. According to the definition of the induction zone of the ZND model, the starting point of the induction zone is the starting point of the leading shock wave, i.e., the starting point of the wedge surface, as shown in Fig. 2(b). Because the flow parameters were changed in this study, the temperature at the end of the ZND model was inconsistent; so the definition of the end point of the induction zone was modified to some extent. In this work, the length of the induction zone is related to the temperature after the shock wave. The end point of the induction zone is defined as the point at which the temperature increases by 10% after the oblique shock wave on the wedge. As shown in Fig. 2(b), the distance between the start and end points of the induction zone is the length of the induction zone, which is expressed by L_C. In this case, L_C = 5.92 mm.

To study the influence of expansion waves on the structures of ODWs, the argon concentration of 50% and the angle of the oblique wedge of 25° are kept unchanged. The characteristic length L_W of the wedge is controlled by changing the inflection point X of the wedge surface, and the temperature contours of ODW structures under different values of L_W are obtained, as shown in Fig. 3. When L_W = 6.07–13.24 mm, as shown in Figs. 3(a)–(c), the flow field is detonated, and, with the decrease of the wedge length, the area of the detonation zone is gradually reduced. The transition type of the oblique shock wave and ODW is abrupt transition, and the position of the transition point is approximately the same. When the wedge length L_W is reduced to 5.52 mm, as shown in Fig. 3(d), the flow field will not be detonated. It can be seen that, under this condition, the length of the induction zone L_C = 5.92 mm, and when the wedge length L_W is greater than 5.92 mm, the ODW will be induced to initiate; otherwise, the ODW will not be initiated.

Fig. 4 presents the distribution curves of the wall temperature and pressure with different lengths of the wedge in Fig. 3. The wall temperature and pressure increase with the airflow passing through the oblique shock wave and combustion wave,

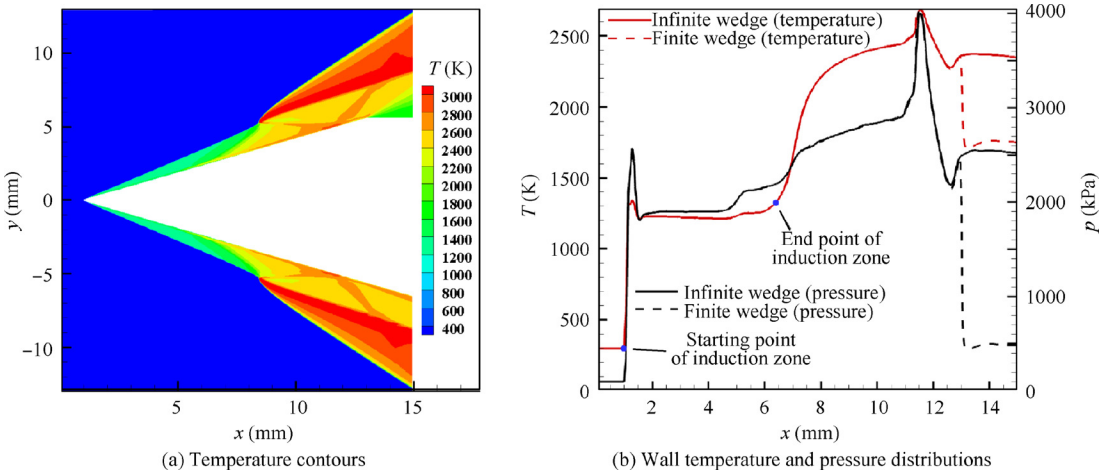

(a) Temperature contours (b) Wall temperature and pressure distributions

Fig. 2 Wave structures, wall temperature and pressure distributions for finite wedge and infinite wedge.

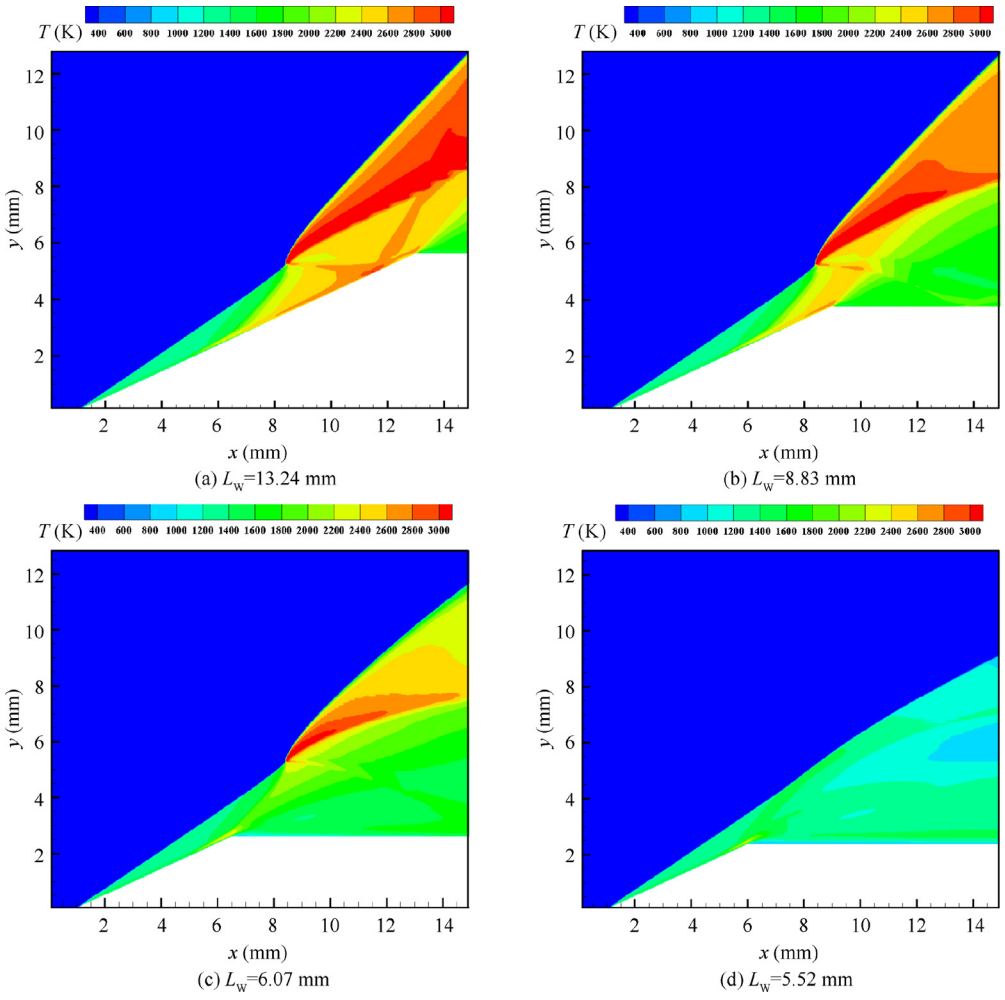

Fig. 3 Temperature contours of ODW structures with different L_W at $Ma_\infty = 7$, $T_\infty = 300$ K, $p_\infty = 101325.0$ Pa, $\theta = 25°$ and 50%Ar.

and decrease with the influence of the expansion wave. It can be seen from the figure that when $L_W = 13.24$ mm, the curves of the wall temperature and pressure suddenly reach the peak values at $x = 11$ mm, which is caused by the transverse shock wave formed at the multi-wave point acting on the wall. Similarly, when $L_W = 8.83$ mm, the curves of the wall temperature and pressure sharply increase at $x = 13.5$ mm, as they are also affected by the transverse shock wave. When $L_W = 6.07$ mm, the effect of the transverse shock on the wall is not obvious. It can be seen from Figs. 3 and 4 that, as the length of the wedge decreases, the greater the influence of the expansion wave, the weaker the strength of the transverse shock wave.

3.2. Effects of argon concentration on ODW

Experimental and numerical investigations on argon dilution have been conducted by researchers and prove the flowfield of oblique detonation more stable.[36] For the ODE,[44–54] the stability of ODWs is significant and the investigation on structures of ODW under argon dilution is necessary. Second, in the real flight condition of ODE at high Mach number, the temperature of air and fuel compressed by the shock is very high. The reduced equivalence ratio and argon dilution are often conduct to prevent the premature combustion. Therefore, this section presents the effects of argon concentration on ODW.

To study the influence of the concentration of argon on the ODW, the wedge length L_W is kept as 13.24 mm and the concentration of argon is varied. The temperature contours of argon concentrations of 40%-80% are obtained, of which the temperature contours of 50% is as shown in Fig. 3(a) above, and the temperature contours of 40%, 60%, 70% and 80% is as shown in Fig. 5. It can be seen from the figure that the oblique detonation is initiated under these five different concentrations. However, the influence of the argon concentration on the initiation characteristics of the ODW is obvious. When the concentration of argon is in the range of 40%-60%, the transition types of the oblique shock wave and ODW are abrupt transition, and the position of the transition point remains approximately the same with the increase of the argon concentration. With the increase of the argon concentration, the transition types of the oblique shock wave and ODW gradually become smooth transition when the concentration reaches 70% and 80%. It is worth noting that when the concentration of argon is 40%, the transverse shock wave interacts with the slip line after reflecting on the wall, and the angle of the shock wave changes. The reflection shock wave

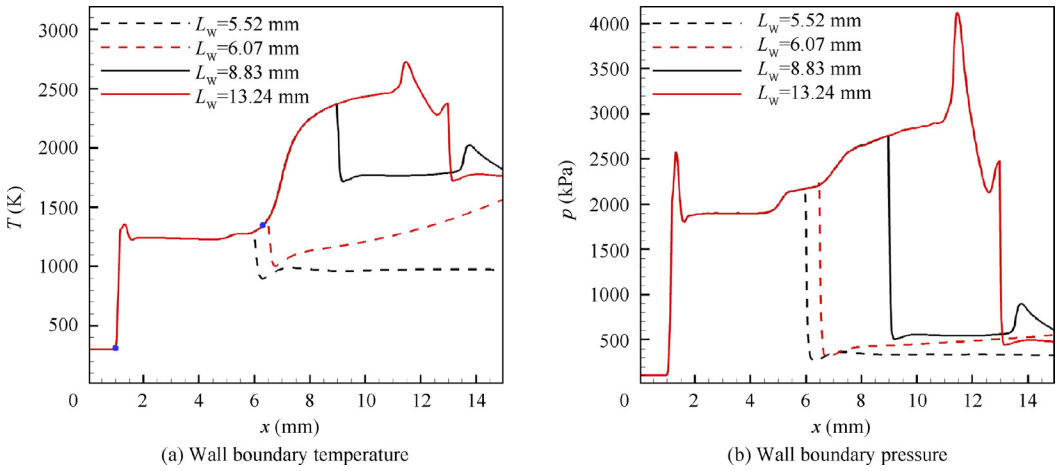

Fig. 4 Temperature and pressure distributions on wall boundary with different L_W at $Ma_\infty = 7$, $T_\infty = 300$ K, $p_\infty = 101325.0$ Pa, $\theta = 25°$ and 50%Ar.

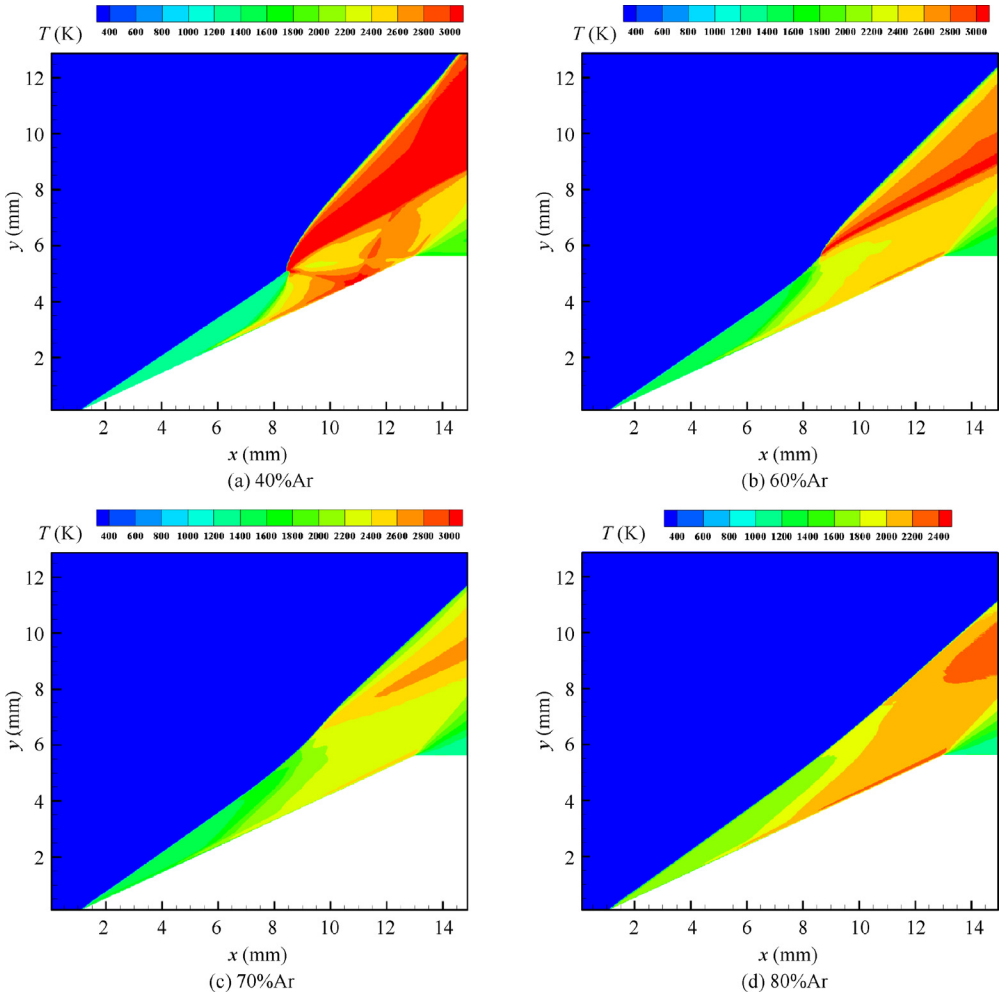

Fig. 5 Temperature contours of ODW structures with different argon concentration at $Ma_\infty = 7$, $T_\infty = 300$ K, $p_\infty = 101325.0$ Pa, $\theta = 25°$ and $L_W = 13.24$ mm.

then interacts with the ODW, resulting in a change of the ODW surface inclination and wave surface instability.

Fig. 6 presents the temperature and pressure distributions along the wall at argon concentrations of 40%-70%. It can be seen from the figure that, with the increase of the argon concentration, the temperature and pressure both increase gradually after the oblique shock and decrease gradually after the expansion wave. When the concentrations of argon are 40% and 50%, a third sharp increase occurs due to the influence of the transverse shock wave. When the argon concentration increases to 60%, as shown in Fig. 5(b), the Mach stem near the detonation wave disappears, the transverse shock wave also disappears, the wave-system structure becomes simpler, and the instability in the ODW band does not occur over a very short distance.

The analytical method based on the CVC theory proposed by Teng et al.[31] is used to predict and measure the theoretical length of the induction zone. This method is realized by establishing a uniform dimension of the length of the induction zone, i.e., the theoretical length is equal to the product of the velocity and theoretical induction time. The mathematical expression is as follows:

$$L_{\text{theory}} = U\tau \tag{4}$$

where U represents the velocity component behind the oblique shock wave moves along the wedge and τ is the theoretical induction time. The parameters T and ρ after the oblique shock wave are introduced[40] to calculate the theoretical induction time corresponding to a 10% temperature increase after the wave. The numerical and theoretical results of the induction zone length at argon concentrations of 0–90% are presented in Fig. 7(a). L_t and L_C represent the theoretical and computational characteristic length of induction zone. It can be seen from the diagram that the type of transition between the oblique shock and ODW is abrupt transition at argon concentrations of 0–60%. Under this condition, the theoretical and numerical results differ greatly. At argon concentrations of 70%–90%, the type of transition between the oblique shock and ODW is smooth transition, and the difference between the theoretical and numerical results is small. As mentioned in previous H_2-air research,[31] smooth transition is referred to as "dynamically-controlled detonation" and abrupt transition is referred to as "wave mechanically-controlled detonation". Therefore, the length of the induction zone of the ODW controlled by dynamics can be calculated by the CVC theory. However, because there is little research and a lack of strict theoretical proof, the error of abrupt transition calculated using the CVC theory is large, and therefore it requires further study.

It can be seen from Section 3.1 that when the wedge length is longer than the length of the numerically calculated induction zone, the ODW can be induced to detonate; otherwise, the ODW cannot be induced to detonate. Therefore, the initiation criteria of the ODW with a finite wedge can be summarized as follows. When the length of the numerically calculated induction zone and the characteristic length of the wedge satisfy $L_C/L_W < 1$, the ODW will be induced to detonate; when $L_C/L_W > 1$, the ODW will not be induced to detonate. Fig. 7(b) presents the initiation of ODWs at different argon concentrations and wedge lengths, in which a hollow triangle represents "not detonated" and a solid triangle represents "detonation." The circle represents the length of the numerically calculated induction zone in the argon concentration range of 10%-80%, and a simple polynomial fitting was performed. The numerical results in Fig. 7(b) further validate the above-mentioned detonation criteria for ODWs.

3.3. Effects of inflow Mach number on ODW

Figs. 8(a) and (b) respectively present the temperature distributions of the flow field at the incoming Mach numbers of Ma_∞ = 8.0, 9.0 under the condition of an infinite wedge and an argon concentration of 50%. Combined with Fig. 2(a), it can be seen that detonation takes place in the flow field at Mach numbers of Ma_∞ = 7.0, 9.0, and an ODW forms. With the increase of the Mach number, the convergence position of the detonation wave moves forward and the induction zone gradually becomes shorter. When Ma_∞ = 7.0, the transition types of the oblique shock surface and oblique detonation surface are abrupt transition, and there are transverse shock and slip lines at the multi-wave points. When Ma_∞ = 8.0–9.0, the transition type becomes smooth transition, the transverse

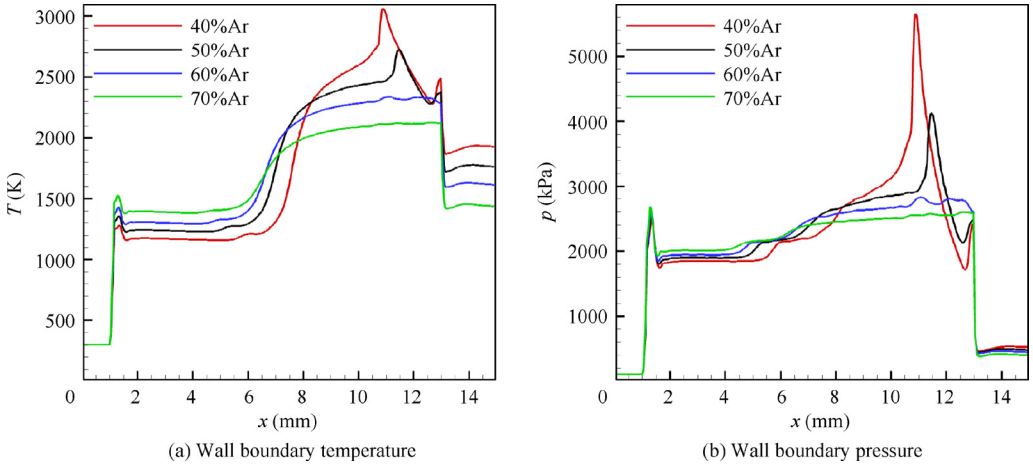

Fig. 6 Temperature and pressure distributions on wall boundary with different argon concentration at Ma_∞ = 7, T_∞ = 300 K, p_∞ = 101325.0 Pa, θ = 25° and L_W = 13.24 mm.

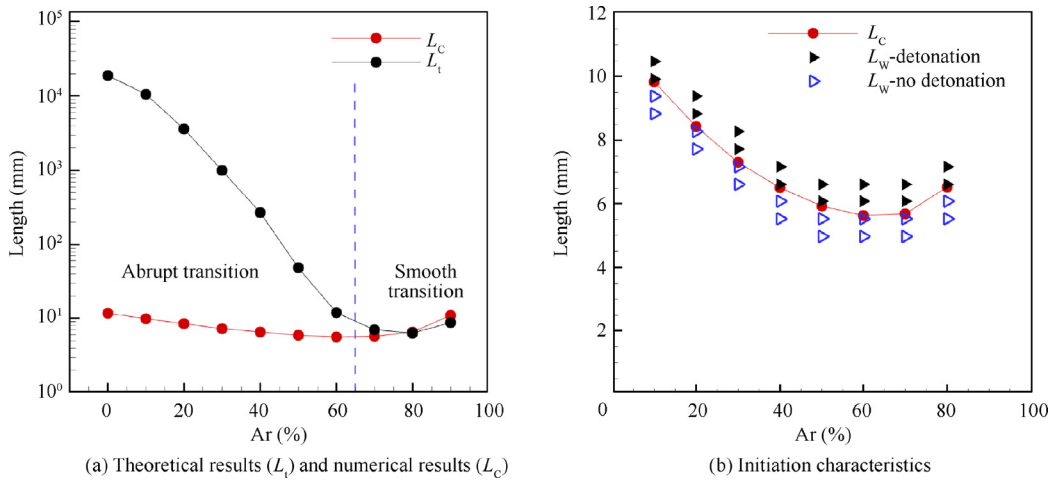

(a) Theoretical results (L_t) and numerical results (L_C) (b) Initiation characteristics

Fig. 7 Characteristic length of oblique detonation with different argon concentration at $Ma_\infty = 7$, $T_\infty = 300$ K, $p_\infty = 101325.0$ Pa, $\theta = 25°$.

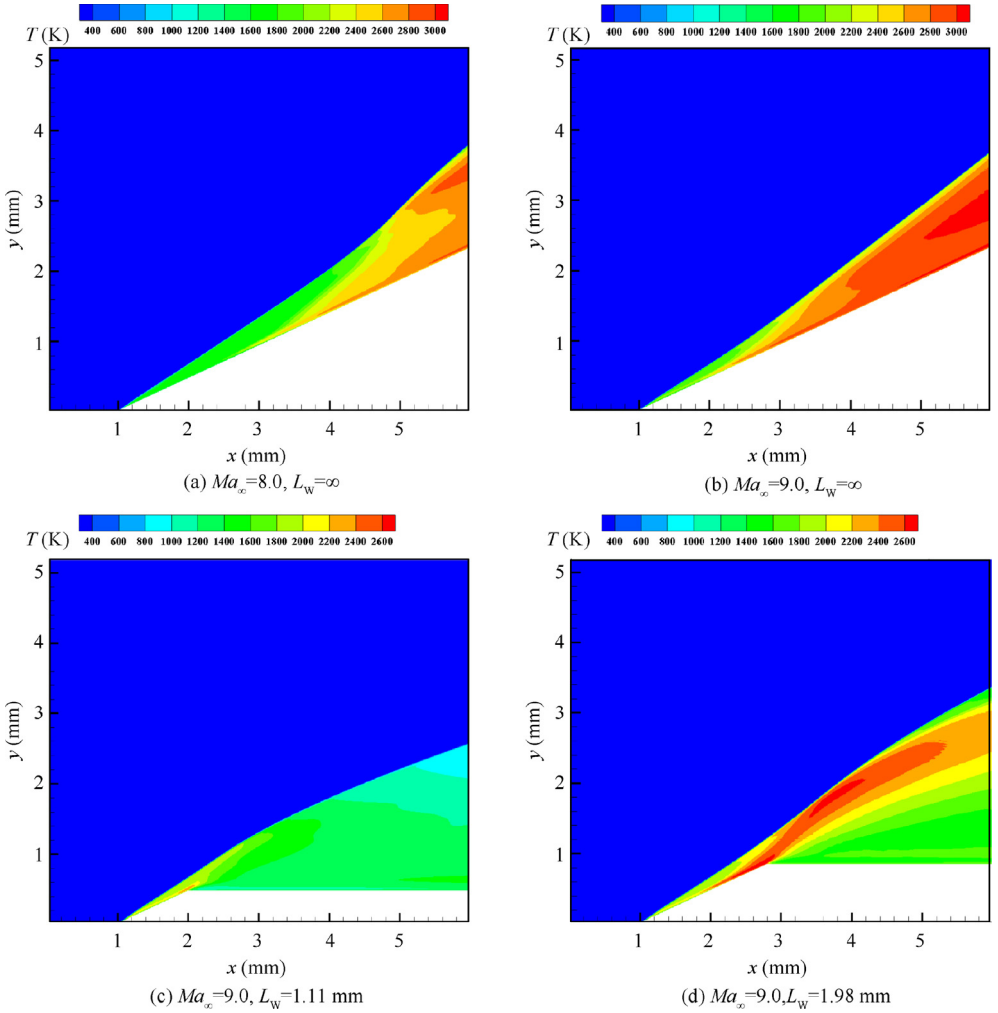

(a) Ma_∞=8.0, L_W=∞ (b) Ma_∞=9.0, L_W=∞

(c) Ma_∞=9.0, L_W=1.11 mm (d) Ma_∞=9.0,L_W=1.98 mm

Fig. 8 Temperature contours of ODW structures with different L_W and Mach number at $T_\infty = 300$ K, $p_\infty = 101325.0$ Pa, $\theta = 25°$ and 50%Ar.

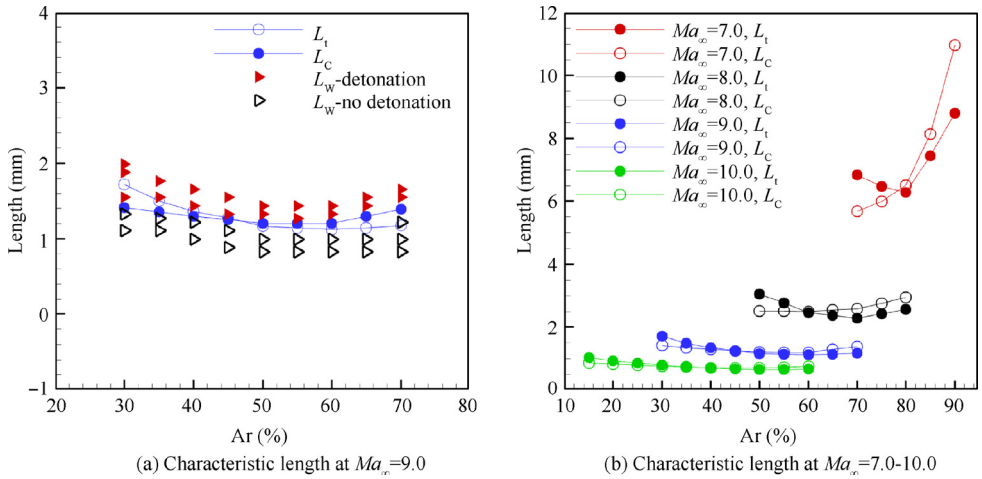

Fig. 9 Characteristic length in different Mach numbers.

shock disappears, the wave-system structure becomes simple, and the flow field becomes more stable. The higher the Mach number, the smoother the transition surface. Figs. 8(c) and (d) present the temperature distributions of the flow field from a finite wedge under an argon concentration of 50%, Ma_∞ = 9.0, and L_W = 1.11, 1.98 mm, respectively. It can be seen from the diagram that when L_W = 1.11 mm < L_C, the flow field does not detonate. When L_W = 1.98 mm > L_C, the flow field detonates and an ODW forms. Fig. 9(a) shows the initiations of ODWs at different argon concentrations and wedge lengths at Ma_∞ = 9.0, where L_t denotes the length of the induction zone calculated by the CVC theory and L_C denotes the length of the numerically calculated induction zone. It can be seen from the diagram that the results at higher Mach numbers also conform to the finite wedge oblique detonation initiation criterion.

Fig. 9 presents the length of the numerically calculated induction zone L_C at the inlet Mach numbers Ma_∞ = 7.0–10.0 and the length of the theoretically calculated induction zone L_t calculated by the CVC theory at different argon concentrations. The error between L_C and L_W in the example in the figure is controlled within 20%, whereas the error of other unsatisfied data exceeds 20%. The following rules can be summarized from the diagram. With the increase of the Mach number, the argon concentration applicable to the CVC theory gradually decreases, and its range gradually extends. The argon concentration is 70%–90% at Ma_∞ = 7.0, 50%–80% at Ma_∞ = 8.0, 30%–70% at Ma_∞ = 9.0, and 15%–60% at Ma_∞ = 10.0. Moreover, with the increase of the Mach number, the error between the lengths of the theoretically and numerically calculated induction zones decreases, and the theoretical solution and numerical solution obtained by the CVC theory fit better. Finally, with the increase of the Mach number, the length of the induction zone changes less with the concentration of argon, which can be observed from the theoretical solution and numerical solution.

4. Conclusions

In this paper, the Euler equations with a detailed chemical model was solved to investigate the oblique detonation induced by a finite wedge under argon dilution. The results show that the expansion waves affect the initiation of the ODW and will extinguish the flow field under certain conditions, which is significant for the design of ODEs.

(1) The main wave structures of the ODWs from the finite wedge and infinite wedge are the same, the expansion waves formed at the inflection point of the wedge affect the downstream flow field behind the inflection point, but has little influence on the upstream flow field before the inflection point.
(2) The increase of the argon concentration and incoming Mach number will change the initiation structure of the ODW from the abrupt type to the smooth type, reduce the wave structure in the initiation zone, and stabilize the flow field. A finite wedge ODW initiation criterion is proposed. When the length L_C of the numerically calculated induction zone and the characteristic length of the wedge L_W satisfy L_C/L_W < 1, the oblique detonation will be initiated; otherwise, it will not be initiated. Many examples were carried out to verify the feasibility of the criterion.
(3) The length of the theoretically calculated induction zone was determined by the CVC theory and compared with the length of the numerically calculated induction zone. It was found that the CVC theory is more suitable for ODW flow fields with a smooth transition type. With the increase of the Mach number, the argon concentration applicable to the CVC theory was found to gradually decrease, the range of the argon concentration gradually broadened and the initiated domain of ODW got larger with different length of L_W. The applicable ranges of CVC theory with different argon concentration at Ma_∞ = 7.0–10.0 were obtained. Therefore, the length of the induction zone can be well predicted and the basis for the design of the engine structure can be provided via combination with the initiation criterion.

Declaration of Competing Interest

The authors declare that they have no known competing financial interests or personal relationships that could have appeared to influence the work reported in this paper.

Acknowledgements

The research is also supported by the Fundamental Research Funds for the Central Universities of China (No. 310201906zy009) and the Basic Research Plan of Natural Science in Shanxi Province—General Project (Youth), China (No. 2019JQ-132).

References

1. Zhang B, Liu H, Yan B, et al. Experimental study of detonation limits in methane-oxygen mixtures: determining tube scale and initial pressure effects. *Fuel* 2020;**259**:116220.
2. Zhang B. Detonation limits in methane-hydrogen-oxygen mixtures: Dominant effect of induction length. *Int J Hydrogen Energ* 2019;**44**:23532–7.
3. Zhang B, Liu H. Theoretical prediction model and experimental investigation of detonation limits in combustible gaseous mixtures. *Fuel* 2019;**258**:116132.
4. Zheng DF, Wang B. Utilization of nonthermal plasma in pulse detonation engine ignition. *J Propul Power* 2018;**34**(2):539–49.
5. Wang YH, Wang JP. Effect of equivalence ratio on the velocity of rotating detonation. *Int J Hydrogen Energ* 2014;**40**(25):7949–55.
6. He W, Xie Q, Ji Z, et al. Characterizing continuously rotating detonation via nonlinear time series analysis. *Proc Combust Inst* 2019;**37**(3):3433–42.
7. Xie Q, Wang B, Wen H, et al. Enhancement of continuously rotating detonation in hydrogen and oxygen-enriched air. *Proc Combust Inst* 2019;**37**(3):3425–32.
8. Fang Y, Zhang Z, Hu Z. Effects of boundary layer on wedge-induced oblique detonation structures in hydrogen-air mixtures. *Int J Hydrogen Energ* 2019;**44**(41):23429–35.
9. Xiang G, Li X, Sun X, et al. Investigations on oblique detonations induced by a finite wedge in high altitude. *Aerosp Sci Technol* 2019;**95**:105451.
10. Huang W, Yan L. Numerical investigation on the ram-scram transition mechanism in a strut-based dual-mode scramjet combustor. *Int J Hydrogen Energ* 2016;**41**(8):4799–807.
11. Huang W. Design exploration of three-dimensional transverse jet in a supersonic crossflow based on data mining and multi-objective design optimization approaches. *Int J Hydrogen Energ* 2014;**39**(8):3914–25.
12. Xiang G, Gao X, Jie X, et al. Flowfield characteristics in sidewall compression inlets. *Acta Mech Sinica* 2020;**36**(3):678–85.
13. Xiang GX, Wang C, Teng HH, et al. Investigations of three-dimensional shock/shock interactions over symmetrical intersecting wedges. *AIAA J* 2016;**54**(5):1472–81.
14. Zhang B, Liu H, Yan B. Investigation on the detonation propagation limit criterion for methane-oxygen mixtures in tubes with different scales. *Fuel* 2019;**239**:617–22.
15. Uy K, Shi LS, Wen CY. Prediction of half reaction length for H_2O_2Ar detonation with an extended vibrational nonequilibrium Zel'dovich-von Neumann-Döring (ZND) model. *Int J Hydrogen Energ* 2019;**44**(14):7667–74.
16. Uy KC, Shi L, Wen C. Chemical reaction mechanism related vibrational nonequilibrium effect on the Zel'dovich- von Neumann-Döring (ZND) detonation model. *Combust Flame* 2018;**196**:174–81.
17. Teng H, Jiang ZL. On the transition pattern of the oblique detonation structure. *J Fluid Mech* 2012;**713**:659–69.
18. Wang Y, Wang J, Li Y, et al. Induction for multiple rotating detonation waves in the hydrogen-oxygen mixture with tangential flow. *Int J Hydrogen Energ* 2014;**39**(22):11792–7.
19. Miao S, Zhou J, Liu S, et al. Formation mechanisms and characteristics of transition patterns in oblique detonations. *Acta Astronaut* 2018;**142**:121–9.
20. Liu Y, Wang L, Xiao B, et al. Hysteresis phenomenon of the oblique detonation wave. *Combust Flame* 2018;**192**:170–9.
21. Xiang GX, Gao X, Tang WJ, et al. Numerical study on transition structures of oblique detonations with expansion wave from finite-length cowl. *Phys Fluids* 2020;**32**(5):056108.
22. Teng H, Ng HD, Li K, et al. Evolution of cellular structures on oblique detonation surfaces. *Combust Flame* 2015;**162**(2):470–7.
23. Li J, Ning J. Experimental and numerical studies on detonation reflections over cylindrical convex surfaces. *Combust Flame* 2018;**198**:130–45.
24. Zhang Y, Fang Y, Ng HD, et al. Numerical investigation on the initiation of oblique detonation waves in stoichiometric acetylene–oxygen mixtures with high argon dilution. *Combust Flame* 2019;**204**:391–6.
25. Qin Q, Zhang X. Study on the effects of geometry on the initiation characteristics of the oblique detonation wave for hydrogen-air mixture. *Int J Hydrogen Energ* 2019;**44**(31):17004–14.
26. Xiang G, Li H, Cao R, et al. Study of the features of oblique detonation induced by a finite wedge in hydrogen-air mixtures with varying equivalence ratios. *Fuel* 2020;**264**:116854.
27. Yang P, Teng H, Ng HD, et al. A numerical study on the instability of oblique detonation waves with a two-step induction–reaction kinetic model. *Proc Combust Inst* 2019;**37**(3):3537–44.
28. Zhang B, Liu H, Li Y. The effect of instability of detonation on the propagation modes near the limits in typical combustible mixtures. *Fuel* 2019;**253**:305–10.
29. Bachman CL, Goodwin GB, Ahmed K. Wedge-stabilized oblique detonation waves in a hypersonic hydrogen-air premixed free-stream. Reston: AIAA; 2019. Report No.: AIAA-2019-4044.
30. Ren Z, Wang B, Xiang G, et al. Effect of the multiphase composition in a premixed fuel-air stream on wedge-induced oblique detonation stabilization. *J Fluid Mech* 2018;**846**:411–27.
31. Fang Y, Hu Z, Teng H, et al. Effects of inflow equivalence ratio inhomogeneity on oblique detonation initiation in hydrogen-air mixtures. *Aerosp Sci Technol* 2017;**71**:256–63.
32. Yang P, Ng HD, Teng H. Numerical study of wedge-induced oblique detonations in unsteady flow. *J Fluid Mech* 2019;**876**:264–87.
33. Li C, Kailasanath K, Oran ES. Detonation structures behind oblique shocks. *Phys Fluids* 1994;**6**(4):1600–11.
34. Viguier C, Silva L, Desbordes D, et al. Onset of oblique detonation waves: comparison between experimental and numerical results for hydrogen-air mixtures. *Symp (Int) Combust* 1996;**26**(2):3023–31.
35. Teng H, Ng HD, Jiang Z. Initiation characteristics of wedge-induced oblique detonation waves in a stoichiometric hydrogen-air mixture. *Proc Combust Inst* 2017;**36**(2):2735–42.
36. Radulescu MI, Ng HD, Lee JHS, et al. The effect of argon dilution on the stability of acetylene-oxygen detonations. *Proc Combust Inst* 2002;**29**(2):2825–31.
37. Ren Z, Wang B, Xiang G, et al. Numerical analysis of wedge-induced oblique detonations in two-phase kerosene-air mixtures. *Proc Combust Inst* 2019;**37**(3):3627–35.
38. Zhang Y, Fang Y, Ng HD, et al. Numerical investigation on the initiation of oblique detonation waves in stoichiometric acetylene-oxygen mixtures with high argon dilution. *Combust Flame* 2019;**204**:391–6.
39. Fang Y, Hu Z, Teng H. Numerical investigation of oblique detonations induced by a finite wedge in a stoichiometric hydrogen-air mixture. *Fuel* 2018;**234**:502–7.
40. Wang T, Zhang Y, Teng H, et al. Numerical study of oblique detonation wave initiation in a stoichiometric hydrogen-air mixture. *Phys Fluids* 2015;**27**(9):096101.
41. Fang Y, Zhang Y, Deng X, et al. Structure of wedge-induced oblique detonation in acetylene-oxygen-argon mixtures. *Phys Fluids* 2019;**31**(2):026108.

42. Kim KH, Kim C, Rho OH. Methods for the accurate computations of hypersonic flows: I. AUSMPW+ scheme. *J Comput Phys* 2001;**174**(1):38–80.
43. McBride BJ, Zehe MJ, Gordon S. NASA Glenn coefficients for calculating thermodynamic properties of individual species. Washington, D.C.: NASA; 2002. Report No.: NASA/TP-2002-211556.
44. Fang YS, Zhang ZJ, Hu ZM, et al. Initiation of oblique detonation waves induced by a blunt wedge in stoichiometric hydrogen-air mixtures. *Aerosp Sci Technol* 2019;**92**:676–84.
45. Zhang B, Liu H, Yan BJ. Effect of acoustically absorbing wall tubes on the near-limit detonation propagation behaviors in a methane-oxygen mixture. *Fuel* 2019;**236**:975–83.
46. Zhang B, Shen X, Pang L, et al. Methane-oxygen detonation characteristics near their propagation limits in ducts. *Fuel* 2016;**177**:1–7.
47. Zhang B, Bai C. Methods to predict the critical energy of direct detonation initiation in gaseous hydrocarbon fuels-an overview. *Fuel* 2014;**117**:294–308.
48. Sun M, Zhao Y, Zhao GY, et al. A conceptual design of shock-eliminating clover combustor for large scale scramjet engine. *Acta Astronaut* 2017;**130**:34–42.
49. Sun M, Zhong Z, Liang J, et al. Experimental investigation on combustion performance of cavity-strut injection of supercritical kerosene in supersonic model combustor. *Acta Astronaut* 2016;**127**:112–9.
50. Huang W, Tan J, Liu J, et al. Mixing augmentation induced by the interaction between the oblique shock wave and a sonic hydrogen jet in supersonic flows. *Acta Astronaut* 2015;**117**:142–52.
51. Huang W, Liu W, Li S, et al. Influences of the turbulence model and the slot width on the transverse slot injection flow field in supersonic flows. *Acta Astronaut* 2012;**73**:1–9.
52. Zhang B, Liu H, Wang C. On the detonation propagation behavior in hydrogen-oxygen mixture under the effect of spiral obstacles. *Int J Hydrogen Energ* 2017;**42**(33):21392–402.
53. Xiang G, Yangi P, Teng H, et al. Cellular aluminum particle-air detonation based on realistic heat capacity model. *Combust Sci Technol* 2020;**192**(10):1931–45.
54. Xiang G, Wang C, Teng H, et al. Shock/shock interactions between bodies and wings. *Chin J Aeronaut* 2018;**31**(2):255–61.